Optics Communications 281 (2008) 5097–5103

Contents lists available at ScienceDirect

Optics Communications

journal homepage: www.elsevier.com/locate/optcom

Chiral photonic crystals with an anisotropic defect layer: Oblique incidence

A.H. Gevorgyan

Physics Department, Yerevan State University, A. Manookian 1, 375025 Yerevan, Armenia

ARTICLE INFO

Article history:
Received 17 October 2007
Received in revised form 23 June 2008
Accepted 9 July 2008

ABSTRACT

In the present paper we consider some properties of defect modes in chiral photonic crystals with an anisotropic defect layer at oblique light incidence. The problem is solved by Ambartsumian's layer addition method. We investigated some peculiarities of the discussed system's reflection spectra of the oblique light incidence for both the minimum and essential influences of the dielectric boundaries. Then we investigated some particulars of the density of photonic states spectra. We also discussed some peculiarities of the light energy distribution in the system. We found out that at large incidence angles two defect modes arise in the two regions of the selective reflection, each in one respectively, meanwhile, none arises in the central region of the complete reflection. Our investigations show that it is possible to rather widely change the emission peak wavelength in the subject system doped with some laser dye, by changing the incidence angle.

1. Introduction

Theoretical and experimental investigations of photonic crystals (PC) have again drawn the attention of the specialists, because the results of such investigations find more and more applications in optoelectronic devices of the new generation. The chiral photonic crystals (CPC) such as cholesteric liquid crystals, chiral smectics and artificial chiral-made crystals and magnetic-chiral PCs, have been of particular interest due to their rich optical properties. The main difference of the chiral photonic crystals (CPCs) from usual PCs is the fact that the photonic band gap (PBG) in CPCs exists only for one circular polarization (at normal incident light), coinciding with the chiral medium helix sign. For these crystals a circular Bragg's reflection occurs between wavelengths $\lambda_1 = \sigma n_o$ and $\lambda_2 = \sigma n_e$, where σ is the pitch of helical structure, and $n_o = \sqrt{\varepsilon_1}$ and $n_e = \sqrt{\varepsilon_2}$ are the ordinary and extraordinary refractive indices of the locally uniaxial structure. The light with opposite circular polarization does not undergo a diffraction reflection. Recently Ross et al. [1] proposed and examined a design strategy to design such ambichiral layered structures, which function reasonably well as rejection filters for nontrivial elliptical polarization states.

The ideal PCs have many applications, but their doped versions are more useful, because they have a greater number of applications, like the doped semiconductors. For instance, introduction of a defect into PC structure gives rise to additional resonance modes inside the PBG. Such defect modes are localized in defect positions and can be used to construct narrow band filters and mirrors (as, in contrast to the ordinary PC, the defect modes aroused in CPC are either narrow transmittance lines in PBG for diffracting circular polarization of the incident light, or they are narrow lines of reflection in the transmittance band for the not diffracting circular polarization of the incident light) and low threshold lasers. Recently, the CPCs having various types of defects have been considered, namely: a thin layer of an isotropic substance installed between two CPC layers [2–7]; a defect caused by a helix phase jump on the boundary of two CPC layers [4,8–10]; a defect caused by a local change of the helix pitch [11–13]; and defects caused by spatially varying helix pitch [14–16]. The CPC with an anisotropic substance layer [17], three-layer system of two chiral-made thin layers with an anisotropic uniaxial layer between them [18–20] is discussed and it was shown that this system's plane wave transmittance spectrum exhibits narrow-stop band characteristics in several wavelength regimes.

In the cited papers the normal light incidence is mainly discussed. In this paper we theoretically investigated peculiarities of the defect modes in a CPC with an anisotropic substance introduced between the two layers of a chiral PC at oblique light incidence and found out some new features of such a system. We also discussed some peculiarities of the light energy distribution in the system. The importance of the present problem is the fact that in contrast to the isotropic defect case, anisotropic defects introduce additional phase differences, which lead to some more interesting peculiarities, as it was shown in [19,20] and some others which we will see below. In particular, as it was shown in [19,20] the defect mode line width becomes depending on the defect layer optical thickness and, because of this and at certain values of the latter, the medium loses its main property, viz. the diffraction reflection polarization dependence. Besides, as it is known, new peculiarities arise at oblique light incidence on a CPC layer.

E-mail address: agevorgyan@ysu.am

0030-4018/$ - see front matter © 2008 Elsevier B.V. All rights reserved.
doi:10.1016/j.optcom.2008.07.024

Let's note that the concept of an anisotropic layer as a phase defect has been explicitly stated by Lakhtakia and Messier in [21], and as it was shown very recently by Lakhtakia in [22], an anisotropic defect layer can actually be a chiral PC, too.

2. The method of analysis

The problem of light propagation through CPC layer at its oblique incidence was solved by different methods. Rokushima and Yamakita [23], and Wang and Lakhtakia [24] exemplify use of the coupled-wave method, Abdulhalim et al. exemplify the use of the Berreman method [25], Belyakov and Dimitrienko provided an approximate analytical method [26,27], and Lakhtakia and Weiglhofer provided an exact analytical method [28], and Polo and Lakhtakia compared the exact analytical method with the Berreman method [29].

Here the problem is solved by the Ambartsumian's layer addition modified method adjusted to solution of problems of the given type (see, for instance, [7]). A CPC with an anisotropic defect can be treated as a three layer system: Two CPC layers, (the CPC(1) and the CPC(2)), and an anisotropic dielectric layer (ADL) between them (or a Fabri–Perrot resonator with diffraction mirrors and an anisotropic dielectric layer filling).

The amplitude of the plane electromagnetic field $\mathbf{E}_\mathrm{i}$ is incident from the left on the system CPC(1)–ADL–CPC(2), and it gives rise reflected $\mathbf{E}_\mathrm{r}$ and transmitted $\mathbf{E}_\mathrm{t}$ fields, respectively. The complex amplitudes of the *incident reflected* and *transmitted* waves with p and s linear polarizations are

$$\mathbf{E}_{\mathrm{i,r,t}} = E^p_{\mathrm{i,r,t}}\mathbf{n}_p + E^s_{\mathrm{i,r,t}}\mathbf{n}_s = \begin{bmatrix} E^p_{\mathrm{i,r,t}} \\ E^s_{\mathrm{i,r,t}} \end{bmatrix}, \tag{1}$$

where $\mathbf{n}_p$, and $\mathbf{n}_s$ are the unit vectors of linear polarizations, and $E^p_{\mathrm{i,r,t}}$ and $E^s_{\mathrm{i,r,t}}$ are the corresponding amplitudes of the incident, reflected and transmitted waves. The reflected and transmitted fields are related to the incident wave by the following way

$$\begin{bmatrix} E^p_r \\ E^s_r \end{bmatrix} = \begin{bmatrix} R_{pp} & R_{ps} \\ R_{sp} & R_{ss} \end{bmatrix} \begin{bmatrix} E^p_\mathrm{i} \\ E^s_\mathrm{i} \end{bmatrix}, \begin{bmatrix} E^p_\mathrm{t} \\ E^s_\mathrm{t} \end{bmatrix} = \begin{bmatrix} T_{pp} & T_{ps} \\ T_{sp} & T_{ss} \end{bmatrix} \begin{bmatrix} E^p_\mathrm{i} \\ E^s_\mathrm{i} \end{bmatrix}, \tag{2}$$

where $\widehat{R}$ and $\widehat{T}$ are the 2×2 matrices of reflectance and transmittance correspondingly. R_{ij} and T_{ij} are the amplitude reflection and transmission coefficients of i-polarized light, assuming that the incident light has a j-polarization.

Let us first compose the reflection and transmission matrices for one helix pitch. To do it we divide the CPC layer of thickness $d = \sigma$ (σ is the helix pitch) into great many thin layers, having the thicknesses: $d_1, d_2, \ldots, d_N$. If the maximum thickness is sufficiently small, one can consider each layer a linear birefringent plate, and take the $d = \sigma$ layer as a stack of parallel and sufficiently small anisotropic layers, each having a principal axis been turned of a small angle $2\pi/N$ in respect to the preceding one.

Then the Ambartsumian's modified layer addition method can be presented in the form of recurrent matrix equations

$$\begin{aligned} \widehat{R}_j &= \hat{r}_j + \hat{\tilde{t}}_j\widehat{R}_{j-1}(\widehat{I} - \hat{\tilde{r}}_j\widehat{R}_{j-1})^{-1}\hat{t}_j, \\ \widehat{T}_j &= \widehat{T}_{j-1}(\widehat{I} - \hat{\tilde{r}}_j\widehat{R}_{j-1})^{-1}\hat{t}_j, \end{aligned} \tag{3}$$

with $\widehat{R}_0 = \hat{0}, \widehat{T}_0 = \widehat{I}$. Here $\widehat{R}_j, \widehat{T}_j, \widehat{R}_{j-1}, \widehat{T}_{j-1}$ are the matrices of reflectance and transmittance for the media with j and (j-1) anisotropic layers, respectively, $\hat{r}_j, \hat{t}_j$ are the analogical matrices for the jth anisotropic layer, $\hat{0}$ is the zero matrix, $\widehat{I}$ is the unit matrix, and the respective matrices for the reverse light propagation are denoted by tilde. Thus, the problem is reduced to finding the matrices of reflectance and transmittance for an anisotropic layer. The solution of this problem is well-known (in the Appendix the exact expressions of the reflectance and transmittance matrices for a birefringent layer are presented, taking into account the Fresnel reflection on the borders). To find the CPC layer reflection and transmission matrices we again use the system of Eq. (1) but we are to take into account that now $\hat{r}_j, \hat{t}_j$ are the matrices of reflectance and transmittance for the $d = \sigma$ CPC layer. We find the matrices of reflectance and transmittance for the CPC(1)–ADL–CPC(2) system in the same way. First, we sew the anisotropic dielectric layer with thickness d' (the layer A) to the layer of CPC(2) (the layer B) from the left. In this case, it is convenient to present the layer addition method in the form of matrix equations:

$$\begin{aligned} \widehat{R}_{\mathrm{A+B}} &= \widehat{R}_\mathrm{A} + \hat{\tilde{T}}_\mathrm{A}\widehat{S}\widehat{T}_\mathrm{A}, \\ \widehat{T}_{\mathrm{A+B}} &= \widehat{T}_\mathrm{B}\widehat{P}\widehat{T}_\mathrm{A}. \end{aligned} \tag{4}$$

Matrices $\widehat{S}$ and $\widehat{P}$ describe the resulting waves that arise in the dielectric layer on the "sewing" plane. So

$$\vec{E}_{\rightarrow} = \widehat{P}\vec{E}_i, \tag{5}$$

is the wave arising on this surface and propagating to the right, and

$$\vec{E}_{\leftarrow} = \widehat{S}\vec{E}_i, \tag{6}$$

is the wave arising on this surface but propagating to the left. Accordingly, the total wave field arising in the dielectric layer on the "sewing" plane has the following form

$$\vec{E}_{\mathrm{total}} = (\widehat{S} + \widehat{P})\vec{E}_i. \tag{7}$$

Accordingly, matrices $\widehat{S}$ and $\widehat{P}$ can be found from the system

$$\begin{aligned} \widehat{S} &= \widehat{R}_\mathrm{B}[\widehat{I} - \hat{\tilde{R}}_\mathrm{A}\widehat{R}_\mathrm{B}]^{-1}, \\ \widehat{P} &= [\widehat{I} - \hat{\tilde{R}}_\mathrm{A}\widehat{R}_\mathrm{B}]^{-1}. \end{aligned} \tag{8}$$

Then we sew the CPC(1) to the anisotropic layer with thickness d'' ($d = d' + d''$ is the thickness of the anisotropic layer) on the left side, too. Finally, we sew these two systems. This procedure makes possible to find the electric field in the anisotropic layer and consequently investigate the light energy distribution in the layer.

Let's note that as the exact solution for the boundary problem of the normal light incidence on a CPC with finite thickness is known, we found the reflectance and transmittance matrices through the exact formulas first and then did the same by the Ambartsumian's layer addition method. Both results almost exactly coincide. Also, the Ambartsumian's layer addition method was checked at the light oblique incidence. The exactness of the fulfilled numerical calculations were controlled by energy (conservation) law (in the absence of absorption $R + T = 1$), and also by comparing obtained results in definite limiting cases with well known earlier results. Note that in our paper [30] were we comparing the approximate analytical method Belyakov and Dimitrienko with the modified Ambartsumian's method.

Let's now turn to the Eigen polarizations (EP) and Eigen amplitudes, as we are to investigate also the reflectance-transmittance peculiarities of subject system in the case of incidence light with EPs. EPs are the two light polarizations, which are not changed if transmitted through the system. These polarizations usually coincide with the normal mode polarizations excited in the system.

Designating the ratio of the field complex amplitudes at the entrance of the system through χ_i ($\chi_i = E^s_i/E^p_i$), and the same ratio at the exit of the system trough χ_t ($\chi_t = E^s_t/E^p_t$), we get their connection from (2):

$$\chi_t = (T_{ss}\chi_i + T_{sp})/(T_{ps}\chi_i + T_{pp}). \tag{9}$$

The function $\chi_t = f(\chi_i)$ is called polarization transfer function [31] and it carries information about the transformation of the polarization ellipse when light transmits trough the system.

Each optical system has two EPs, which are obtained by the substitution $\chi_i = \chi_t$. According to (9) we get for EPs χ_1 and χ_2:

$$\chi_{1,2} = \frac{T_{ss} - T_{pp} \pm \sqrt{(T_{ss} - T_{pp})^2 + 4T_{ps}T_{sp}}}{2T_{ps}}. \tag{10}$$

The function

$$F(\chi_i) = \sqrt{\frac{(|T_{ps}\chi_i + T_{pp}|^2 + |T_{ss}\chi_i + T_{sp}|^2)}{(1 + |\chi_i|^2)}} \frac{(T_{ps}\chi_i + T_{pp})}{|T_{ps}\chi_i + T_{pp}|}, \tag{11}$$

is called the transfer function for the complex amplitude of the transmitted wave [31]. The transfer function's eigen values for the transmitted wave complex amplitudes $V_1 = F(\chi_1)$ and $V_2 = F(\chi_2)$ which correspond to its EPs, define the transmittance amplitude coefficients at the incidence of light with the polarizations $\chi_i = \chi_1$ and $\chi_i = \chi_2$, respectively.

Similarly, the function

$$G(\chi_i) = \sqrt{\frac{(|R_{ps}\chi_i + R_{pp}|^2 + |R_{ss}\chi_i + R_{sp}|^2)}{(1 + |\chi_i|^2)}} \frac{(R_{ps}\chi_i + R_{pp})}{|R_{ps}\chi_i + R_{pp}|}, \tag{12}$$

is called the transfer function for the complex amplitude of the reflected wave. The transfer function's eigen values for the reflected wave complex amplitude, $W_1 = G(\chi_1)$ and $W_2 = G(\chi_2)$, which correspond to its EPs, define the reflectance amplitude coefficients at the incidence of light with the polarizations $\chi_i = \chi_1$ and $\chi_i = \chi_2$, respectively.

3. Results and discussion

If the system contains an anisotropic defect layer, then the change of the layer's optical thickness leads to the change of the defect mode line width [19,20]. Below we present the results of the defect mode peculiarities at defect layer small optical thickness–when light energy accumulation in the system takes place. In such a situation, the system can work as a narrow band filter or mirror; also such a system can be used for creating low-threshold lasers. The reflection spectra at various incident angles are presented in Fig. 1. The first column shows the reflection coefficient dependence on the wavelength both for the right handed (the blue solid curve) and left handed (the red dotted

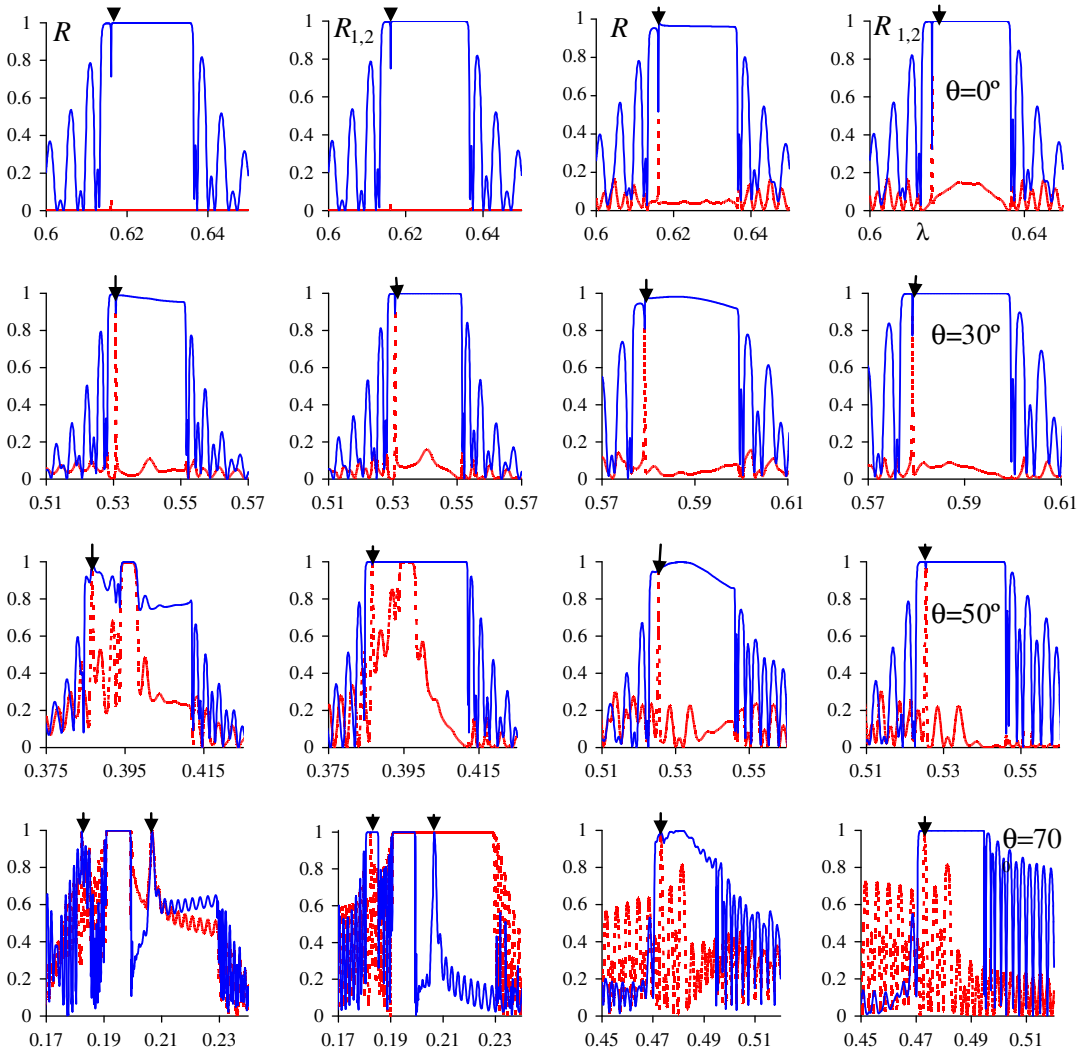

Fig. 1. Plots of the reflection spectra at various incidence angles. The first column shows the reflection coefficient dependence on the wavelength both for the right handed (the blue solid curve) and left handed (the red dotted curve) circularly polarized light incidence. The second column shows the reflection coefficient dependence on the wavelength for the first (the blue solid curve) and second (the red dotted curve) EP light incidence ($R_{1,2} = |W_{1,2}|^2$). The CPC screw is right handed. Both columns present the case of dielectric borders minimum influence, i.e. the case for $\varepsilon_m = \varepsilon$. The third and forth columns show the analogous dependences for the case $\varepsilon = 1$. The defect is at the centre of the system. The CPC layer parameters are: $\varepsilon_1 = 2.29$, $\varepsilon_2 = 2.143$, $\sigma = 0.42$ μm, $L = 100\sigma$, and the defect layer parameters are: $\varepsilon_1^d = 2.317$, $\varepsilon_2^d = 3.048$; the defect layer thickness is $d = 0.028$ μm. (For interpretation of the references to colour in this figure legend, the reader is referred to the web version of this article.)

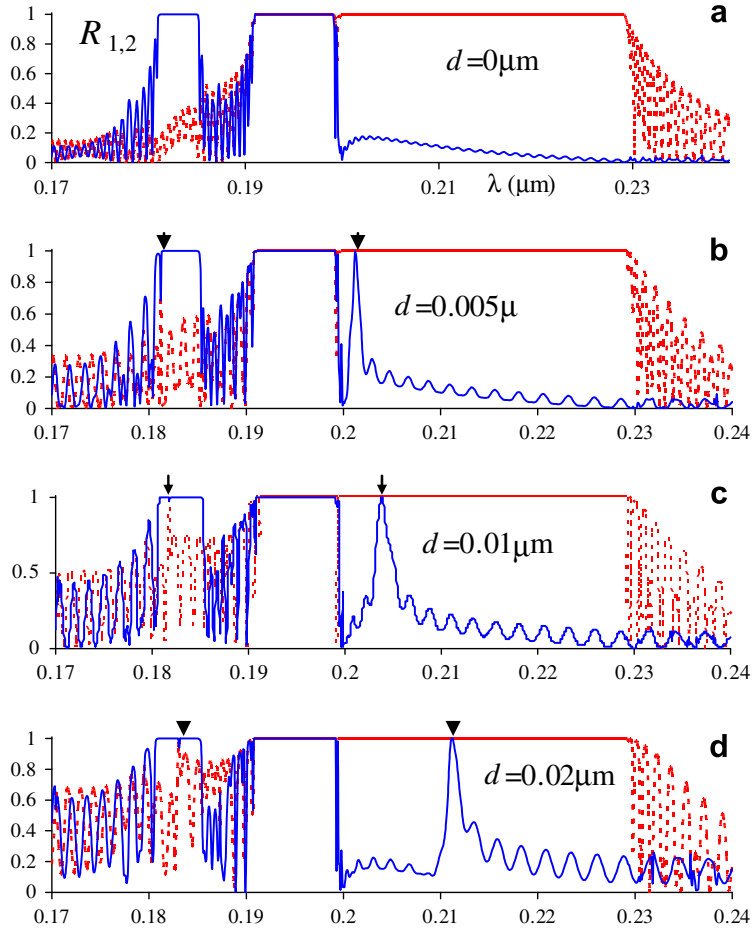

Fig. 2. Plots of the reflection coefficients $R_{1,2}$ versus wavelength λ for a defect layer of various thicknesses d for the case of oblique light incidence (at $\theta = 70°$). Parameters are the same as in Fig. 1. (For interpretation of the references to color in this figure, the reader is referred to the web version of this article.)

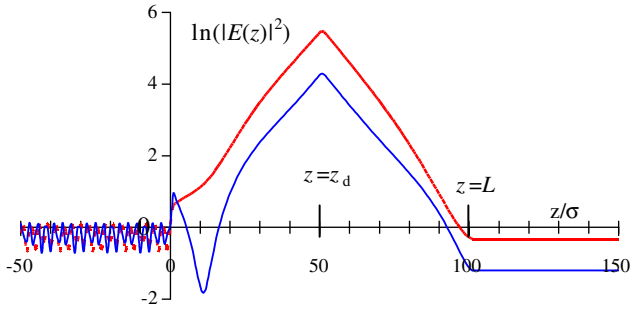

Fig. 3. Plots logarithmical intensity $\ln(|E(z)|^2)$ versus z (the axis z coincides with the medium axis) at the normal light incidence. The CLC layer occupies the region $0 \leqslant z \leqslant L$ ($L = 100\sigma$), the defect is at the CLC center and the defect center is at the $z = z_d = 50\sigma$. The parameters are the same as in Fig. 1. (For interpretation of the references to color in this figure, the reader is referred to the web version of this article.)

curve) circularly polarized light incidence. The second column shows the reflection coefficient dependence on the wavelength for the first (the blue solid curve) and second (the red dotted curve) EP light incidence ($R_{1,2} = |W_{1,2}|^2$). Both columns present the case of dielectric borders' minimum influence, i.e. the case for $\varepsilon_m = \varepsilon$ ($\varepsilon_m = \frac{\varepsilon_1+\varepsilon_2}{2}$, $\varepsilon_1, \varepsilon_2$ are the CPC permittivity tensor's principal values, ε is the permittivity of the medium enclosing the CPC layer with defect inside it.) And the third and forth columns show the analogous dependences for the case $\varepsilon = 1$, when the CPC layer is in the air and the dielectric borders influence is significant. The CPC helix is a right handed one.

In contrast to the normal incidence, qualitatively new peculiarities arise in CPC optics in the case of oblique incidence. In this case there are reflections of higher orders at frequencies multiple to the Bragg frequency. Besides, in this case, the both EP waves become diffraction waves (one of them is strong acting and the other is weak acting). And at large incidence angles, a total reflection region (not selective in respect to the polarization) is formed. Let us note that such an effect was predicted by Belyakov and Dmitrienko [26,27] and it was experimentally established in [32,33]. At larger incidence angles a three peak diffraction region is formed, having a central total reflection region and two side regions of selective reflection. These regions can either border with each other, or be separate, depending on the incident angle and the parameters of the problem. The peculiarities of the ideal (without any defect) CPC reflection spectra and the dielectric borders' influence on those spectra were discussed in detail in [30]. The comparison of the spectra of the present paper to the analogous ones for CPCs with ideal periodical structures of [30] and to the spectra for CPCs with an anisotropic defect layer at normal incidence of [20] shows that the incidence angle increase leads to:

(1) some increase of the defect mode line width,
(2) some increase of reflection for the weakly interacting EP wave and a decrease of the transmission of the strongly interacting EP wave, both at the defect mode wavelength.

At normal incidence, such changes take place if the defect layer optical thickness increases. The incidence angle increase also leads to the effective optical thickness' increase. An interesting situation arises at larger incidence angles if the influence of the dielectric borders is minimum (i.e. if a three peak diffraction region is formed, having a central total reflection region and two side regions of selective reflection.) In Fig. 2 the reflection spectra for various defect layer thicknesses are presented for the case of oblique incidence (at $\theta = 70°$, θ is the angle of incidence). And in Fig. 2a the reflection spectrum of the non-defect case is brought to compare to the defect having ones (i.e., compared to Fig. 2b–d). As it is seen, the defect does not lead to significant changes of the central total reflection region. Some defect modes appear in the selective reflection side regions. An increase of the defect layer thickness leads to the defect modes line width change and their shift into PBGs. Defect modes appear in the selective reflection short wave region for the both EP of the incidence wave, but they appear only for the strongly interacting EP of the incidence wave in the long wave region. Let us note that the defect mode also appears for only one mode in CLC with locally deformed helix [11].

As it is known, a CPC doped with laser dyes (resonance atoms) can be used to create feedback lasers, without using any mirror. In the amplifying media (for instance, in CPCs doped with fluorescent guest-molecules, but for the case that the fluorescenting peak is either in the PBG, or covers it), the PBG significantly influences on the radiation spectrum. The wave is evanescent (decreases exponentially) in the PBG and consequently the spontaneous radiation vanishes. The explanation is that the photonic density of states (PDS) vanishes, and as the spontaneous radiation intensity is proportional to PDS [34,35], the spontaneous radiation intensity also vanishes. Indeed, according to the theory developed in [34,35], the spontaneous radiation intensity at the point z of the layer is found as follows:

$$p(\lambda, z) = \frac{\rho_m(\omega)}{\rho_{\text{iso}}} \frac{\langle |\mathbf{d}|^2 \rangle |E_m(z)|^2}{U(k)}, \tag{13}$$

where ρ_m and $E_m(z)$ are the PDS and electric field of mth EP, ρ_{iso} is the PDS of an isotropic homogeneous layer with a refraction coefficient $n = \sqrt{\varepsilon}$, $\langle |\mathbf{d}|^2 \rangle$ is the dipole transition momentum averaged in respect to the orientation distribution, $U(k)$ is the total electric energy accumulated in the CPC. At PBG borders the spontaneous radiation life time τ_s sharply increases (τ_s decreases with oscillations outside it) and makes the stimulated radiation strongly go up.

In the experiments of the laser beam generation in a dye-doped CPC the ideal periodic structure without any defects the lasing always occurs at the lower-energy edge of the PBG. According to Araoka and Shin [36], it is due to the following circumstances. It is known that at the short wave (long wave) border of the PBG in CPC, the diffraction mode total electric field is linearly polarized, which is perpendicular (parallel) to the local director. The low threshold lasing can be realized by the single mode selection. The polymeric dye used in the said experiments gives highly ordered arrangement along the molecular director, because of the dipole interactions. Consequently, the emission transmission moments of the monomeric units align along the same direction. Then the emission mode may be selected. Of course, the lasing can occur at the higher-energy edge of PBG, too [37,44].

As the CPC helix pitch can be changed and also be tuned, a possibility of tuning the laser radiation wavelength arises, which has most important practical significance.

The effects of the electric field, temperature, light radiation and defects on the dye-doped CPC lasing performance have been studied [36–49].

Yablonovitch has predicted that a low-threshold lasing will occur at defect modes within the band gap of PCs too, since the excitation energy is not drained by spontaneous emission into modes other than the lasing mode [50]. Lasing is further facilitated at the wavelength of the defect mode since the photon dwell time is enhanced, giving ample opportunity for amplification by stimulated emission. Below we investigate the relative PDS spectra peculiarities and the light energy distribution peculiarities in the system. We are investigating possibilities of tuning the emission peak wavelength by the incidence angle change.

In Fig. 3 the dependence of $\ln(|E(z)|^2)$ on z (the axis z coincides with the medium axis) at the normal light incidence is presented. The CLC layer occupies the region $0 \leqslant z \leqslant L$ ($L = 100\sigma$), the defect is at the CLC center and the defect center is at the $z = z_d = 50\sigma$. As it follows from the Figure, the maximum of $|E(z)|^2$ is at the defect center.

In Fig. 4 the spectra of $\frac{\rho_m(\lambda)}{\rho_{iso}}$ are presented in the case of dielectric borders minimum influence, i.e., the case for $\varepsilon_m = \varepsilon$ (a–d) and in the

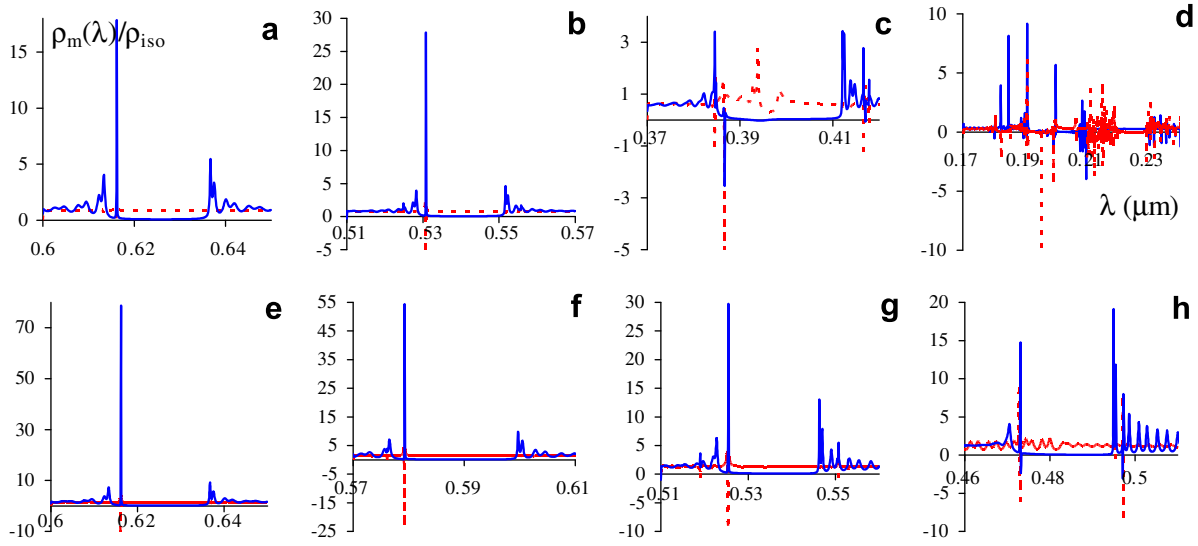

Fig. 4. The dependence of $\frac{\rho_m(\lambda)}{\rho_{iso}}$ on the wavelength at the following incidence angles: $\alpha = 0°$ (a,e), $\alpha = 30°$ (b,f), $\alpha = 50°$ (c,g) и $\alpha = 70°$ (d,h) and in cases if the dielectric borders influence is minimum (a–d) and the system is in vacuum i.e. in the case $\varepsilon = 1$ (e–h). The incidence light is the first (the blue solid curve) and second (the red dotted curve) EP. The parameters are the same as in Fig. 1. (For interpretation of the references to colour in this figure legend, the reader is referred to the web version of this article.)

case $\varepsilon = 1$, i.e. the case when the dielectric borders influence is significant (e–h) for various incidence angles.

The density of states $\rho(\omega)$ is the inverse of the group velocity and is given by [52,53]

$$\rho(\omega) \equiv \frac{\mathrm{d}k}{\mathrm{d}\omega} = \frac{1}{L}\frac{v\frac{\mathrm{d}u}{\mathrm{d}\omega} - u\frac{\mathrm{d}v}{\mathrm{d}\omega}}{v^2+u^2} \tag{14}$$

where v and u are the real and imaginary parts of the transmission coefficients, respectively.

As it can be seen from Fig. 4, $\frac{\rho_m(\lambda)}{\rho_{\mathrm{iso}}}$ ($\rho_m(\lambda) = \frac{\mathrm{d}\omega}{\mathrm{d}\lambda}\rho_m(\omega)$) has maximums on the PBG borders and at defect mode wavelength and at certain circumstances the second one is much higher than the first one. Here a low-threshold lasing appears because of light energy abundant accumulation at the defect location at the defect mode.

The presented results show that there is one more possibility of tuning the emission peak wavelength in CLC, namely, changing the incidence angle. If this angle increases, both $\frac{\rho_m(\lambda)}{\rho_{\mathrm{iso}}}$ at its maximum and its peak frequency location change. And if the dielectric borders influence is minimum, the number of maximums of $\frac{\rho_m(\lambda)}{\rho_{\mathrm{iso}}}$ increases (consequently, the number of wavelengths, at which emission has peaks, increases), because, as it is mentioned above, at the oblique incidence a complicated three-peak diffraction region appears; besides, at larger incidence angles the diffraction modes appear in both regions of the selective diffraction reflection. But at larger incidence angles the relative PDS, $\frac{\rho_m(\lambda)}{\rho_{\mathrm{iso}}}$ maximums decrease. When the dielectric borders influence is minimum, the lasing wavelength changes within a rather large interval, but the incident angle increase significantly decreases the maximums of $\frac{\rho_m(\lambda)}{\rho_{\mathrm{iso}}}$. In contrast to these, when the dielectric borders' influence is significant, the lasing wavelength changes in a comparatively smaller interval, but the above mentioned maximums are relatively stable in respect to incident angle changes.

4. Conclusion

Summing up, let us note that in the present paper we have investigated defect mode peculiarities in CLC with an anisotropic defect inside. CLC with anisotropic defects can be created, for instance, on the base of cholesteric liquid crystals (CLC). Liquid crystals (LC), containing chiral molecules, have a self organizing helicoidal structure, and these media are 1D CLC. And, as liquid crystals can be easily tuned, it is possible to create an anisotropic defect inside the CLC layer and tune its location, for instance, by a static external electric field created by a series of electrodes arranged along the CLC axis. Then the defect layer thickness will be defined by the electrode longitudinal dimensions and the applied voltage. Besides, applying voltage to different pairs of electrodes, one can change the defect location inside the system.

We showed that at large incidence angles and at the minimum influence of the dielectric boundaries, two defect modes arise in the system – each one in the two regions of the selective reflection, respectively – provided that such a three peak diffraction reflection region is aroused, which has a complete reflection region with sided regions of the selective reflection.

We also investigated the possibility of tuning the emission peak wavelength in a CLC layer with an anisotropic defect doped with a laser dye. We showed that one can change the emission peak wavelength in a sufficiently large wavelength range by changing the incident wave angle.

Acknowledgements

This work was supported in part by Armenian National Science and Educational Fund (Grant #1264-PS). The author is grateful to the Referees for useful remarks.

Appendix

Let us consider light propagation through a one-axis crystal with its optical axis parallel to the boundary surfaces, and having the angle ϕ with x-axis of the laboratory system. The incidence plane coincides with the (x,z) plane, and the z-axis is directed along the normal of the crystal's surface, the y axis is perpendicular to light incidence plane, and the incidence angle is θ. The dielectric permittivity tensor of such a layer has the following form:

$$\hat{\varepsilon} = \varepsilon_m \begin{pmatrix} 1+\delta\cos 2\phi & \delta\sin 2\phi & 0 \\ \delta\sin 2\phi & 1-\delta\cos 2\phi & 0 \\ 0 & 0 & 1-\delta \end{pmatrix}, \tag{A1}$$

where $\varepsilon_m = \frac{\varepsilon_1+\varepsilon_2}{2}$, $\delta = \frac{\varepsilon_1-\varepsilon_2}{\varepsilon_1+\varepsilon_2}$, ε_1 and ε_2 – are the crystal's dielectric permittivity values along its optical axis and along the direction perpendicular to that axis, respectively. We are considering a non-magnetic crystal and take $\mu \equiv 1$. Solving the wave equation for such a crystal, we get the following dispersion equation for k_z:

$$\begin{aligned} &k_z^4 - 2k_z^2\left[\frac{\omega^2}{c^2}\varepsilon_m - k_x^2\frac{1-\delta\sin^2\phi}{1-\delta}\right] + k_x^4\frac{1+\delta\cos 2\phi}{1-\delta} \\ &- 2\frac{\omega^2}{c^2}\varepsilon_m(1+\delta\cos^2\phi)k_x^2 + \frac{\omega^4}{c^4}\varepsilon_m^2(1-\delta^2) = 0, \end{aligned} \tag{A2}$$

where $k_x = \frac{\omega}{c}n_0\sin\theta$, n_0 – is the reflection coefficient of the medium having borders with subject layer at its both sides. The solutions of this equation are:

$$\begin{aligned} k_{z1,2} &= \pm\frac{\omega}{c}n_{1,2} = \pm\frac{\omega}{c}\sqrt{\varepsilon_m(1-\delta-\eta^2\sin^2\theta)}, \\ k_{z3,4} &= \pm\frac{\omega}{c}n_{3,4} = \pm\frac{\omega}{c}\sqrt{\varepsilon_m\left(1+\delta-\eta^2\frac{1+\delta\cos 2\phi}{1-\delta}\sin^2\theta\right)}, \end{aligned} \tag{A3}$$

where $\eta = n_0/\sqrt{\varepsilon_m}$.

Solving the reflection and transmission problems of this layer for the reflection and transmission matrix elements $\hat{r}, \hat{t}$, we get (also see [51]):

$$\begin{aligned} r_{11} &= [(h_{11}-h_{21})(h_{32}+h_{42}) - (h_{12}-h_{22})(h_{31}+h_{41})]/\Delta, \\ r_{12} &= 2\cos\theta(h_{31}h_{42}-h_{32}h_{41})/\Delta, \\ r_{21} &= -2(h_{11}h_{22}-h_{12}h_{21})/(\Delta\cos\theta), \\ r_{22} &= [(h_{31}-h_{41})(h_{12}+h_{22}) - (h_{32}-h_{42})(h_{11}+h_{21})]/\Delta, \\ t_{11} &= 2\cos\theta(h_{32}-h_{42})/\Delta, \\ t_{12} &= -2\cos\theta(h_{31}+h_{41})/\Delta, \\ t_{21} &= -2(h_{12}+h_{22})/\Delta, \\ t_{22} &= 2(h_{11}+h_{21})/\Delta, \end{aligned} \tag{A4}$$

where:

$$\begin{aligned} h_{11} &= P_1\cos\theta + n_0P_2, \quad h_{12} = P_3 + n_0\cos\theta P_4, \\ h_{21} &= (P_5\cos\theta + n_0P_1)\cos\theta/n_0, \\ h_{22} &= (P_6 + n_0\cos\theta P_7)\cos\theta/n_0, \\ h_{31} &= P_7\cos\theta + n_0P_4, \quad h_{32} = P_8 + n_0\cos\theta P_9, \\ h_{41} &= (\cos\theta P_6 + n_0P_3)/(n_0\cos\theta), \\ h_{42} &= (P_{10} + n_0\cos\theta P_3)/(n_0\cos\theta), \\ P_1 &= (\varepsilon_2\cos^2\phi\cos b_1 + n_1^2\sin^2\phi\cos b_3)/a, \\ P_2 &= \mathrm{i}n_1\left(\cos^2\phi\sin b_1 + \frac{n_1^3}{n_3\varepsilon_2}\sin^2\phi\cos b_3\right)/a, \\ P_3 &= n_1^2\sin\phi\cos\phi(\cos b_1 - \cos b_3)/a, \\ P_4 &= \mathrm{i}\sin\phi\cos\phi\left(n_1\sin b_1 - \frac{n_1^2}{n_3}\sin b_3\right)/a, \\ P_5 &= \mathrm{i}\varepsilon_2\left(\frac{\varepsilon_2}{n_1}\cos^2\phi\sin b_1 + n_3\sin^2\phi\sin b_3\right)/a, \\ P_6 &= \mathrm{i}\varepsilon_2\sin\phi\cos\phi(n_1\sin b_1 - n_3\sin b_3)/a, \end{aligned}$$

$$P_7 = \varepsilon_2 \sin\phi\cos\phi(\cos b_1 - \cos b_3)/a,$$
$$P_8 = (n_1^2 \sin^2\phi\cos b_1 + \varepsilon_2\cos^2\phi\cos b_3)/a,$$
$$P_9 = \mathrm{i}(n_1\sin^2\phi\sin b_1 + \frac{\varepsilon_2}{n_3}\cos^2\phi\sin b_3)/a,$$
$$P_{10} = \mathrm{i}(n_1^3\sin^2\phi\sin b_1 + \varepsilon_2 n_3\cos^2\phi\sin b_3)/a, \quad \text{(A5)}$$

$a = \varepsilon_2 - n_0^2\sin^2\theta\sin^2\phi, b_i = k_i d, i = 1,\ldots,4$, d – the layer thickness.

References

[1] B.M. Ross, A. Lakhtakia, I.J. Hodgkinson, Opt. Commun. 259 (2006) 479.
[2] Y.-C. Yang et al., Phys. Rev. E 60 (1999) 6852.
[3] I.J. Hodgkinson et al., Opt. Commun. 210 (2002) 201.
[4] J. Schmidtke, W. Stille, Eur. Phys. J. E 12 (2003) 553.
[5] I.J. Hodgkinson et al., Phys. Rev. Lett. 91 (2003) 223903-4.
[6] A.H. Gevorgyan, J. Contemp. Phys. (Acad. Sci. Arm). 40 (2005) 32.
[7] A.H. Gevorgyan, A. Kocharian, G.A. Vardanyan, Opt. Commun. 259 (2006) 455.
[8] V.I. Kopp, A.Z. Genack, Phys. Rev. Lett. 89 (2002) 033901.
[9] J. Schmidtke, W. Stille, H. Finkelmann, Phys. Rev. Lett. 90 (2003) 083902.
[10] M. Becchi, S. Ponti, J.A. Reyes, C. Oldano, Phys. Rev. B70 (2004) 033103.
[11] T. Matsui, M. Ozaki, K. Yoshino, Phys. Rev. E 69 (2004) 061715.
[12] R. Ozaki et al., Jpn. J. Appl. Phys. 45 (1B) (2006) 493.
[13] A.V. Shabanov, S.Ya. Vetrov, A.Yu. Korneev, JETF Lett. 80 (2004) 181.
[14] J.-Y. Chen, L.-W. Chen, J. Phys. D: Appl. Phys. 30 (2005) 1118.
[15] J.-Y. Chen, L.-W. Chen, Phys. Rev. E71 (2005) 061708.
[16] J.-Y. Chen, L.-W. Chen, J. Opt. A: Pure Appl. Opt. 7 (2005) 558.
[17] M.H. Song et al., Adv. Mater. 16 (2004) 779.
[18] A. Lakhtakia et al., Opt. Commun. 177 (2000) 57.
[19] A.H. Gevorgyan, Tech. Phys. Lett. 32 (2006) 698.
[20] A.H. Gevorgyan, M.Z. Harutyunyan, Phys. Rev. E 76 (2007) 031701.
[21] A. Lakhtakia, R. Messier, Sculptured Thin Films: Nanoengineered Morphology and Optics, SPIE Press, Bellingham, WA, USA, 2005.
[22] A. Lakhtakia, Opt. Commun. 275 (2007) 283.
[23] K. Rokushima, J. Yamakita, J. Opt. Soc. Am. 73 (1983) 901.
[24] F. Wang, A. Lakhtakia, Opt. Commun. 235 (2004) 133.
[25] I. Abdulhalim, L. Benguigui, R. Weil, J. Phys. France 46 (1985) 815.
[26] V.A. Belyakov, V.D. Dmitrienko, Sov. Phys. Sol. State 15 (1974) 1811.
[27] V.D. Dmitrienko, V.A. Belyakov, Sov. Phys. Sol. State 15 (1974) 2365.
[28] A. Lakhtakia, W.S. Weiglhofer, Microw. Opt. Technol. 12 (1996) 245.
[29] J.A. Polo, A. Lakhtakia, Microw. Opt. Technol. Lett. 35 (2002) 397.
[30] A.H. Gevorgyan, Opt. Spectrosc. 105 (2) (2008) 317.
[31] R.M.A. Azzam, N.M. Bashara, Ellipsometry and Polarized Light, North-Holland, Amsterdam, 1977.
[32] H. Takazoe, Y. Ouchi, et al., Jpn. J. Appl. Phys. 22 (1983) 1080.
[33] H. Takazoe, Y. Ouchi, M. Hara, et al., Jpn. J. Appl. Phys. 21 (1982) L390.
[34] K.L. Woon, M. O'Neill, G.J. Richards, M.P. Aldred, S.M. Kelly, Phys. Rev. E 71 (2005) 041706.
[35] J. Schmidtke, W. Stille, Eur. Phys. J. B 31 (2003) 179.
[36] F. Araoka, K.-Ch. Shin, et al., J. Appl. Phys. 94 (2003) 279.
[37] S. Furumi, S. Yokoyama, A. Otomo, S. Mashiko, Appl. Phys. Lett. 82 (2003) 16.
[38] S.M. Morris, A.D. Ford, M.N. Pivnenko, H.J. Coles, J. Appl. Phys. 97 (2005) 023103.
[39] A. Chanishvili, G. Chilaya, G. Petriashvili, Appl. Phys. Lett. 83 (2003) 5353.
[40] A.F. Muñoz, P. Palffy-Muhoray, B. Taheri, Opt. Lett. 26 (2001) 804.
[41] Y. Huang, Y. Zhou, Sh.-T. Wu, Appl. Phys. Lett. 88 (2006) 011107.
[42] G. Strangi, V. Barna, et al., Phys. Rev. Lett. 94 (2005) 063903.
[43] Y. Huang, Y. Zhou, et al., Opt. Commun. 261 (2006) 91.
[44] H.M. Song, K.-Ch. Shin, et al., Sci. Technol. Adv. Mater. 5 (2004) 437.
[45] H. Finkelmann, S.T. Kim, et al., Adv. Mater. 13 (2001) 1069.
[46] A. Chanishvili, G. Chilaya, G. Petriashvili, et al., Adv. Mater. 16 (2004) 791.
[47] R. Ozaki, T. Matsui, M. Ozaki, K. Yoshino, Appl. Phys. Lett. 82 (2003) 3593.
[48] P.V. Shibaev, R.L. Sanford, et al., Opt. Express 13 (2005) 2358.
[49] P.V. Shibaev, V.I. Kopp, A.Z. Genack, J. Phys. Chem. 107 (2003) 6961.
[50] E. Yablonovitch, Phys. Rev. Lett. 58 (1987) 2059.
[51] H. Wohler, M. Fritsch, G. Haas, D.A. Mlynski, J. Opt. Soc. Am. A 8 (1991) 536.
[52] J.M. Bendickson, J.P. Dowling, M. Scalora, Phys. Rev. E 53 (1996) 4107.
[53] J.P. Dowling, J. Lightwave Technol. 17 (1999) 2142.